

Showcasing joint research from Pohang University of Science and Technology (POSTECH), Republic of Korea, and Tokyo Institute of Technology (TIT), Japan.

Selective dual-purpose photocatalysis for simultaneous H_2 evolution and mineralization of organic compounds enabled by a Cr_2O_3 barrier layer coated on Rh/SrTiO_3

Dual-purpose photocatalysis for H_2 evolution with the simultaneous mineralization of 4-chlorophenol can be achieved under de-aerated conditions using a $\text{Cr}_2\text{O}_3/\text{Rh}/\text{SrTiO}_3$ photocatalyst, which has Rh nanoparticles covered by a thin Cr_2O_3 barrier layer to selectively control the dual-function surface redox reactions.

As featured in:



See Wonyong Choi *et al.*,
Chem. Commun., 2016, **52**, 9636.



www.rsc.org/chemcomm

Registered charity number: 207890



Cite this: *Chem. Commun.*, 2016, 52, 9636

Received 20th May 2016,
Accepted 28th June 2016

DOI: 10.1039/c6cc04260k

www.rsc.org/chemcomm

Selective dual-purpose photocatalysis for simultaneous H₂ evolution and mineralization of organic compounds enabled by a Cr₂O₃ barrier layer coated on Rh/SrTiO₃†

Young-Jin Cho,^a Gun-hee Moon,^a Tomoki Kanazawa,^b Kazuhiko Maeda^b and Wonyong Choi^{*a}

Dual-functional photocatalysis for H₂ evolution with the simultaneous mineralization of 4-chlorophenol was achieved under de-aerated conditions using a Cr₂O₃/Rh/SrTiO₃ photocatalyst which has Rh nanoparticles covered with a thin Cr₂O₃ barrier layer to selectively control and maximize the dual-functional photocatalytic activity.

Hydrogen is considered as an ideal energy storage medium and a promising energy carrier since it can be obtained from abundant natural resources such as water and biomass instead of fossil fuels.^{1–4} In particular, photocatalytic water splitting is widely studied as a promising technology to produce hydrogen using solar light.^{5–7} Another important application of photocatalysis is the degradation of organic compounds for the remediation of polluted water and air.^{8–12} In photocatalytic H₂ production, organic electron donors are commonly used as sacrificial agents to scavenge photogenerated holes.^{13–17} However, the intentional addition of organic electron donors (e.g., alcohols, organic acids, amines) for H₂ production is not practically acceptable since the electron donors themselves are another energy resource (often more expensive than H₂). Therefore, a more desirable strategy is to use organic waste and pollutants in water as *in situ* electron donors. This is the concept of dual-functional photocatalysis which produces H₂ along with the simultaneous degradation of organic pollutants.^{18–20} Recently, Kim *et al.* demonstrated that the simultaneous H₂ production with the anoxic photocatalytic degradation of organic compounds can be achieved by using TiO₂ modified by both surface fluorination and Pt deposition (F-TiO₂/Pt).^{19,20}

However, the total organic carbon (TOC) removal efficiency was negligible and TOC remained almost unchanged during the photocatalytic degradation of 4-chlorophenol (4-CP) on F-TiO₂/Pt, because dioxygen was needed for mineralization. Meeting the optimal condition for dual-purpose photocatalysis is contradictory because the H₂ evolution requires anoxic conditions whereas the mineralization of organic compounds needs dioxygen.

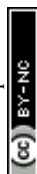
In this study, a selective dual-purpose photocatalysis that achieves H₂ production and TOC removal simultaneously under anoxic conditions is reported. Instead of using the combination of TiO₂ (as a base photocatalyst) and Pt (as a cocatalyst for H₂ evolution), SrTiO₃ (base photocatalyst) and Rh@Cr₂O₃ core-shell nanostructure (cocatalyst) were employed in this work. The photocatalytic activities of the composite materials of Cr₂O₃/Pt/SrTiO₃ and other Rh@Cr₂O₃ (core-shell) loaded metal oxides have been previously demonstrated for the overall water splitting.^{21,22} In this work, we demonstrate that Cr₂O₃/Rh/SrTiO₃ can be a promising dual-purpose photocatalyst that can produce H₂ along with TOC removal (mineralization) of aromatic pollutants in a de-aerated aqueous suspension which is considered an inappropriate condition to achieve the mineralization of organic pollutants.

Cr₂O₃/Rh/SrTiO₃ photocatalyst was prepared by step-wise photo-deposition of Rh nanoparticles on the SrTiO₃ surface as a core and then the Cr₂O₃ nano-shell on the Rh core.²² The loading amount of Rh and Cr₂O₃ was 0.5 wt% and 0.75 wt%, respectively. Fig. S1 (ESI†) shows the HRTEM images of Cr₂O₃/Rh/SrTiO₃ and Rh/SrTiO₃ photocatalysts. Rh nanoparticles of 2–4 nm diameter were observed to be deposited on the surface of both photocatalysts and the Cr₂O₃ shell was seen around the Rh core of the Cr₂O₃/Rh/SrTiO₃ catalyst. Rh/SrTiO₃ and Cr₂O₃/Rh/SrTiO₃ were compared for the photocatalytic degradation of 4-CP under de-aerated conditions as shown in Fig. 1. Cr₂O₃/Rh/SrTiO₃ exhibited a much higher activity than Rh/SrTiO₃ in both the removal of 4-CP and the concurrent production of chloride (Fig. 1a). The TOC removal was also highly enhanced with Cr₂O₃/Rh/SrTiO₃ (Fig. 1b). These results clearly indicate that the removal of 4-CP in the suspension of Cr₂O₃/Rh/SrTiO₃ proceeded along with the mineralization

^a School of Environmental Science and Engineering, Pohang University of Science and Technology (POSTECH), Pohang, 790-784, Republic of Korea.
E-mail: wchoi@postech.edu

^b Department of Chemistry, School of Science, Tokyo Institute of Technology,
2-12-1-NE-2 Ookayama, Meguro-ku, Tokyo 152-8550, Japan

† Electronic supplementary information (ESI) available: Experimental details of the synthesis of Rh/SrTiO₃, Cr₂O₃/Rh/SrTiO₃ and F-TiO₂/Pt, experimental details of photocatalytic reaction and photoelectrochemical tests, and Fig. S1–S7. See DOI: 10.1039/c6cc04260k



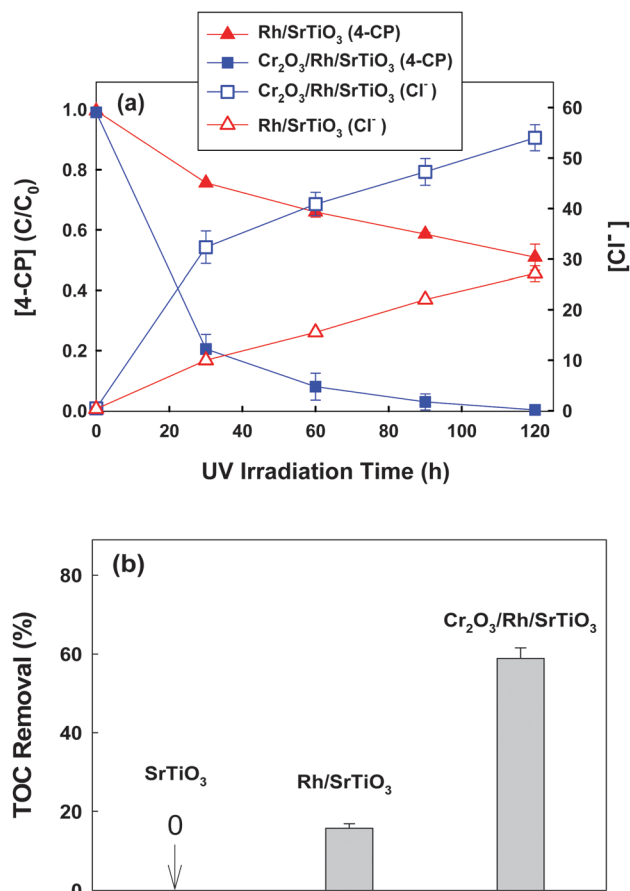


Fig. 1 (a) Photocatalytic degradation of 4-CP and the concurrent production of chloride in a de-aerated catalyst suspension. (b) Comparison of TOC removal efficiencies after 2 h photocatalytic reaction. Experimental conditions: [catalyst] = 0.5 g L⁻¹, [4-CP]₀ = 100 μM, pH₀ = 7, λ > 320 nm, air-tight, and initially Ar-purged for 1 h before UV irradiation.

(i.e., TOC removal) even under the de-aerated conditions, where the initial dissolved O₂ was measured to be less than 0.1 ppm using a dissolved O₂ meter. In the absence of O₂ that serves as a main electron scavenger, the photocatalytic oxidation and mineralization should be inhibited on a bare semiconductor but the loading of Rh and Cr₂O₃ changes the photocatalytic reaction mechanism.

H₂ evolution was also monitored during the anoxic degradation of 4-CP. As seen in Fig. 2a, markedly increased H₂ production was observed with the Cr₂O₃/Rh/SrTiO₃ photocatalyst compared with Rh/SrTiO₃. The initial rate of H₂ production on Cr₂O₃/Rh/SrTiO₃ was around 12 μmol h⁻¹. The apparent photonic efficiency of H₂ evolution (with 300 μM 4-CP) was separately measured under the irradiation centered around λ = 330 ± 10 nm and determined to be 0.7%. Concurrent O₂ evolution was also observed in the case of Cr₂O₃/Rh/SrTiO₃, whereas no O₂ production was observed with Rh/SrTiO₃. Such a difference can be ascribed to the fact that the Cr₂O₃ layer over Rh can suppress the back reaction of H₂ with O₂ to produce H₂O.²³ The fact that O₂ was evolved along with the degradation of 4-CP on Cr₂O₃/Rh/SrTiO₃ indicates that holes react with both 4-CP and water molecules. The *in situ* generated O₂ should be subsequently consumed during the

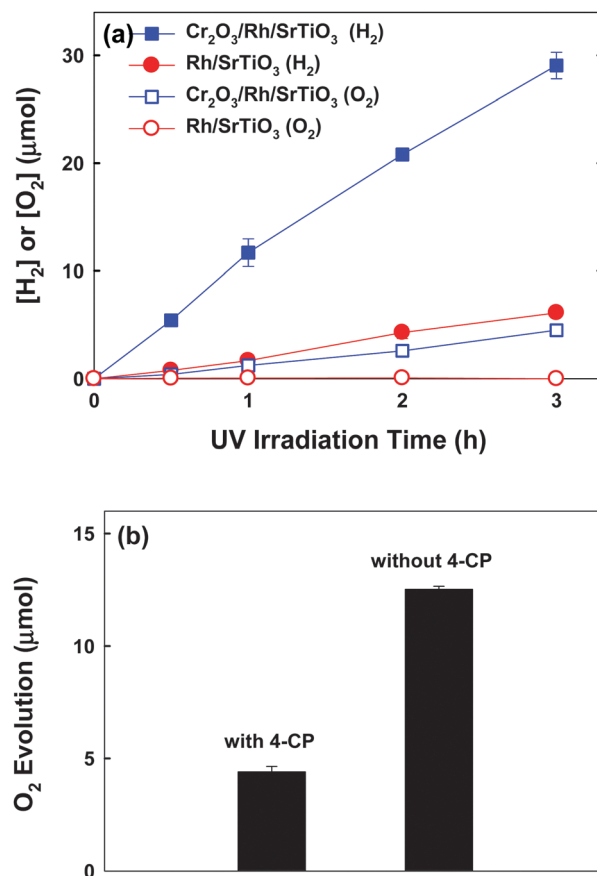
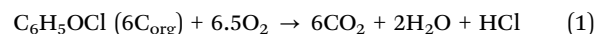
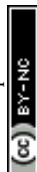


Fig. 2 (a) Time-profiled production of H₂ and O₂ in the suspension of Cr₂O₃/Rh/SrTiO₃ and Rh/SrTiO₃ with 4-CP (300 μM) in the initially de-aerated suspension. (b) Comparison of photocatalytic O₂ evolution in the suspension of Cr₂O₃/Rh/SrTiO₃ (after 3 h reaction) in the presence and absence of 4-CP.

mineralization of 4-CP,^{19,24,25} which explains why the degradation of 4-CP was possible under de-aerated conditions. As a result, the *in situ* O₂ evolution was significantly enhanced in the absence of 4-CP (Fig. 2b). The mineralization of 4-CP can be expressed by eqn (1).



During the initial stage (for 1 h) of photo-irradiation, the rates of H₂ and O₂ evolution were determined to be around 12 μmol h⁻¹ and 1.2 μmol h⁻¹, respectively. The O₂ evolution rate is much lower than the expected stoichiometric rate (6 μmol h⁻¹) in the dual-purpose photocatalysis, which should be ascribed to the *in situ* consumption of O₂ in the mineralization (as mentioned above). In this case, the average TOC removal rate was 5.0 μmol h⁻¹, which corresponds to 5.4 μmol h⁻¹ of the O₂ consumption rate (according to eqn (1)). Therefore, the sum of the apparent O₂ evolution (1.2 μmol h⁻¹) and the *in situ* consumption of O₂ (5.4 μmol h⁻¹) is 6.6 μmol h⁻¹, which is close to the stoichiometric O₂ evolution rate of 6.0 μmol h⁻¹. Incidentally, from a practical point of view, dual-functional photocatalysts working under air-saturated conditions would be desirable. Therefore, H₂ evolution in an aerated suspension of Cr₂O₃/Rh/SrTiO₃ was



also tested. As shown in Fig. S2 (ESI[†]), H₂ evolved even under air-saturated conditions although they were lower compared with Ar-saturated conditions. This result indicates that this composite photocatalyst can be effectively used for dual-functional photocatalysis in both the presence and absence of dissolved O₂.

The effects of dissolved O₂ and the probe reagents (*i.e.*, *t*-butyl alcohol (TBA) and EDTA) were further investigated to understand the photocatalytic mechanisms of Cr₂O₃/Rh/SrTiO₃ and Rh/SrTiO₃, as shown in Fig. S3 (ESI[†]). First, it is noted that the effects of dissolved O₂ are drastically different between Cr₂O₃/Rh/SrTiO₃ and Rh/SrTiO₃. The presence and absence of O₂ did not affect the 4-CP degradation on Cr₂O₃/Rh/SrTiO₃ at all while the degradation of 4-CP on Rh/SrTiO₃ was significant only in the presence of O₂. This observation is fully consistent with the previous reports that the Cr₂O₃ shell layer covering the Rh core blocks the contact of O₂ with the Rh core, but is still permeable to protons.^{22,23} As a result, the CB electron transfer to O₂ on Cr₂O₃/Rh/SrTiO₃ is insignificant but the CB electron transfer to protons (H⁺) is allowed with enabling the concurrent hole transfer to 4-CP. Fig. S3 (ESI[†]) also shows that the photocatalytic degradation of 4-CP remains unchanged in the presence of excessive TBA (as an OH radical scavenger) but is highly retarded in the presence of excessive EDTA (as a hole scavenger).²⁶ This supports that 4-CP degradation proceeds *via* a direct hole-transfer, and not an OH radical-mediated pathway.

To investigate the role of the Cr₂O₃ shell on the Rh core and its effects on the interfacial electron transfer on Cr₂O₃/Rh/SrTiO₃ and Rh/SrTiO₃, the Fe^{3+/2+} redox couple-mediated photocurrent was collected (*via* reactions (2) and (3)) in the UV-irradiated suspension of each catalyst.²⁷

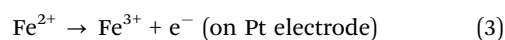
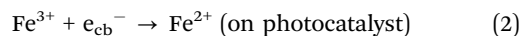


Fig. S4 (ESI[†]) shows that the time profile of photocurrent generation is completely suppressed by Cr₂O₃/Rh/SrTiO₃ in comparison with Rh/SrTiO₃, which is the opposite to the photocatalytic activity of H₂ evolution. This result reconfirms that the Cr₂O₃ layer on the Rh core suppresses the interfacial electron transfer to Fe³⁺ ions as it hinders the electron transfer to O₂ molecules. The presence of the Cr₂O₃ layer blocks the CB electron transfer to electron acceptors (*e.g.*, O₂, Fe³⁺) except protons. On the other hand, holes generated on Cr₂O₃/Rh/SrTiO₃ are mostly consumed by water molecules with generation of O₂, which enables the anoxic degradation of 4-CP. As a result, the photocatalytic production of H₂ on Cr₂O₃/Rh/SrTiO₃ under the de-aerated conditions depended little on the presence and kind of organic electron donors (see Fig. S5, ESI[†]). The photocatalytic H₂ production rates on Cr₂O₃/Rh/SrTiO₃ only moderately changed among the different conditions of water, 10 vol% MeOH, and 300 μM 4-CP whereas the electron donor effect on H₂ production was very critical for Rh/SrTiO₃. This implies that the photocatalytic production of H₂ with the simultaneous decomposition of organic pollutants can be achieved effectively in the Cr₂O₃/Rh/SrTiO₃ photocatalytic system regardless of the kind and concentration of organic pollutants.

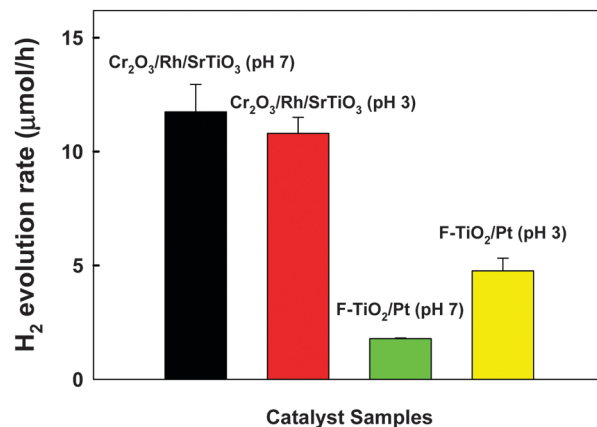
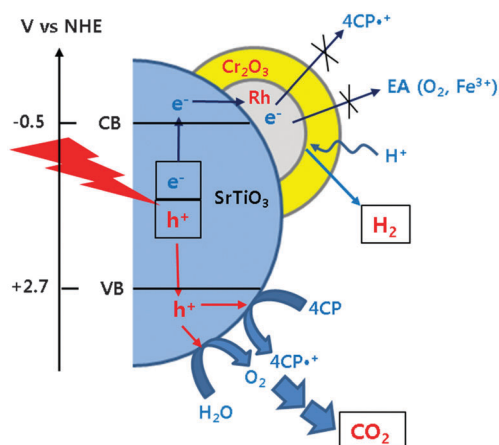


Fig. 3 Comparison of the initial photocatalytic H₂ production rate between Cr₂O₃/Rh/SrTiO₃ and F-TiO₂/Pt photocatalytic systems in the presence of 4-CP (300 μM). Experimental conditions: [catalyst] = 0.5 g L⁻¹, λ > 320 nm, air-tight and initially Ar-purged for 1 h before UV irradiation.

Our recent studies demonstrated that the TiO₂ modified with both Pt and fluoride (F-TiO₂/Pt) exhibited a dual-functional photocatalytic activity for the simultaneous production of H₂ and degradation of 4-CP.^{19,20} In Fig. 3, the H₂ production on Cr₂O₃/Rh/SrTiO₃ was compared with F-TiO₂/Pt under neutral and acidic pH conditions. The photocatalytic activity of Cr₂O₃/Rh/SrTiO₃ is higher than that of F-TiO₂/Pt and less affected by the pH change. It should be noted that the activity of F-TiO₂/Pt is markedly reduced at neutral pH whereas that of Cr₂O₃/Rh/SrTiO₃ was little influenced by pH. As a result, Cr₂O₃/Rh/SrTiO₃ is a better dual-functional photocatalyst from a practical point of view. In terms of the charge transfer characteristics, the following two major features make Cr₂O₃/Rh/SrTiO₃ a practical dual-functional photocatalyst. For the electron transfer part, CB electrons are selectively consumed by protons only and their transfer to O₂ and other electron acceptors (EA) is hindered because the Cr₂O₃ barrier layer is selectively permeable only to protons. On the other hand, VB holes are utilized to oxidize both H₂O (to O₂) and 4-CP (organic pollutants) simultaneously and the *in situ* generated O₂ is immediately consumed for the mineralization of the organic pollutants.^{19,24,28} The reaction mechanisms described above are schematically illustrated in Scheme 1. In the absence of the Cr₂O₃ layer, the CB electrons can be consumed by not only protons but also *in situ* generated O₂ and other reaction intermediates, which would reduce the overall dual-photocatalysis activity.

To check the photostability of Cr₂O₃/Rh/SrTiO₃, the photocatalytic H₂ production was repeated up to four cycles in the same batch of catalyst by injecting 100 μM 4-CP every 2 h (Fig. S6, ESI[†]). The activity was not maintained and gradually decreased with repeated uses. To elucidate whether the gradual loss of activity was caused by the instability of the photocatalyst, the same experiment was performed without 4-CP injection. In this case, the photocatalytic activity was maintained without showing activity loss. The composite photocatalyst itself seems to be stable. Therefore, the gradual loss of photocatalytic activity observed in the presence of 4-CP might be ascribed to





Scheme 1 Schematic illustrations of photocatalytic reaction mechanisms occurring on the surface of $\text{Cr}_2\text{O}_3/\text{Rh}/\text{SrTiO}_3$.

the accumulation of organic degradation intermediates on the catalyst surface.^{29,30} To further investigate the effect of organic compounds in this dual functional photocatalysis, the evolution of H_2 and O_2 was simultaneously measured with repeated photocatalysis cycles. In this case, 100 μM 4-CP was initially added but not replenished in the subsequent cycles. Fig. S7 (ESI[†]) shows that H_2 production was higher in the first cycle than in the subsequent cycles: the difference in H_2 production should be ascribed to the organic electron donor (*i.e.*, 4-CP) effect. The extra holes scavenged by 4-CP make an equal number of electrons to be used for H_2 production. At the same time, O_2 evolved in the first cycle is immediately consumed for the mineralization of 4-CP. As a result, the ratio of H_2 to O_2 in the first cycle was significantly higher ($\text{H}_2/\text{O}_2(r) = 6.9$) than the stoichiometric water splitting ratio ($r = 2.0$). The ratio progressively approached the stoichiometric ratio as the cycle was repeated ($r: 6.9 \rightarrow 2.7 \rightarrow 2.5 \rightarrow 2.2$).

In conclusion, this study demonstrated that the mineralization of organic pollutants can be achieved under the de-aerated conditions with the simultaneous H_2 production over a $\text{Cr}_2\text{O}_3/\text{Rh}/\text{SrTiO}_3$ photocatalyst. The present study showed the highest H_2 evolution efficiency in dual-purpose photocatalysis to our knowledge. It is proposed that the Cr_2O_3 shell on the Rh nanoparticle core markedly enhances the H_2 production and TOC removal of aromatic pollutants, which makes $\text{Cr}_2\text{O}_3/\text{Rh}/\text{SrTiO}_3$ an active dual-functional photocatalyst.

This work was supported by the Global Research Laboratory (GRL) Program (NRF-2014K1A1A2041044), the Global Frontier R&D Program on Center for Multiscale Energy System (2011-0031571), and KCAP (Sogang Univ.) (No. 2009-0093880) funded by the Korea government (MSIP) through the National Research Foundation

of Korea (NRF). K. M. acknowledges a Grant-in-Aid for Young Scientists (A) (Project 25709078) and the PRESTO/JST program "Chemical Conversion of Light Energy" for funding support.

References

- G. Zhang, C. Ni, X. Huang, A. Welgamage, L. A. Lawton, P. K. J. Robertson and J. T. S. Irvine, *Chem. Commun.*, 2016, **52**, 1673.
- M. Ni, D. Y. C. Leung and M. K. H. Leung, *Int. J. Hydrogen Energy*, 2007, **32**, 3238–3247.
- F. Sastre, M. Oteri, A. Corma and H. Garcia, *Energy Environ. Sci.*, 2013, **6**, 2211.
- Y. Tachibana, L. Vayssieres and J. R. Durrant, *Nat. Photonics*, 2012, **6**, 511.
- A. Kudo and Y. Miseki, *Chem. Soc. Rev.*, 2009, **38**, 253.
- Y. Ma, X. Wang, Y. Jia, X. Chen, H. Han and C. Li, *Chem. Rev.*, 2014, **114**, 9987.
- T. Hisatomi, J. Kubota and K. Domen, *Chem. Soc. Rev.*, 2014, **43**, 7520.
- H. Park, Y. Park, W. Kim and W. Choi, *J. Photochem. Photobiol., C*, 2013, **15**, 1.
- M. R. Hoffmann, S. T. Martin, W. Choi and D. W. Bahnemann, *Chem. Rev.*, 1995, **95**, 69.
- Q. Xiang, J. Yu and M. Jaroniec, *Chem. Soc. Rev.*, 2012, **41**, 782.
- J. Yang, R. Hu, W. Meng and Y. Du, *Chem. Commun.*, 2016, **52**, 2620.
- H. Park, H.-i. Kim, G.-h. Moon and W. Choi, *Energy Environ. Sci.*, 2016, **9**, 411.
- X.-Y. Zhang, H.-P. Li, X.-L. Cui and Y. Lin, *J. Mater. Chem.*, 2010, **20**, 2801.
- M.-C. Wu, J. Hiltunen, A. Sápi, A. Avila, W. Larsson, H.-C. Liao, M. Huuhtanen, G. Tóth, A. Shchukarev, N. Laufer, A. Kukovecz, Z. Kónya, J.-P. Mikkola, R. Keiski, W.-F. Su, Y.-F. Chen, H. Jantunen, P. M. Ajayan, R. Vajtai and K. Kordás, *ACS Nano*, 2011, **5**, 5025.
- P. Gomathisankar, K. Hachisuka, H. Katsumata, T. Suzuki, K. Funasaka and S. Kaneco, *Int. J. Hydrogen Energy*, 2013, **38**, 11840.
- W. Zhang, Y. Wang, Z. Wang, Z. Zhong and R. Xu, *Chem. Commun.*, 2010, **46**, 7631.
- M. Wen, Y. Kuwahara, K. Mori, D. Zhang, H. Li and H. Yamashita, *J. Mater. Chem. A*, 2015, **3**, 14134.
- Y.-J. Cho, H.-i. Kim, S. Lee and W. Choi, *J. Catal.*, 2015, **330**, 387.
- J. Kim and W. Choi, *Energy Environ. Sci.*, 2010, **3**, 1042.
- J. Kim, D. Monllor-Satoca and W. Choi, *Energy Environ. Sci.*, 2012, **5**, 7647.
- K. Maeda, A. Xiong, T. Yoshinaga, T. Ikeda, N. Sakamoto, T. Hisatomi, M. Takashima, D. Lu, M. Kanehara, T. Setoyama, T. Teranishi and K. Domen, *Angew. Chem., Int. Ed.*, 2010, **49**, 4096.
- K. Maeda, K. Teramura, D. Lu, N. Saito, Y. Inoue and K. Domen, *Angew. Chem., Int. Ed.*, 2006, **45**, 7806.
- M. Yoshida, K. Takanabe, K. Maeda, A. Ishikawa, J. Kubota, Y. Sakata, Y. Ikezawa and K. Domen, *J. Phys. Chem. C*, 2009, **113**, 10151.
- D. Hufschmidt, D. Bahnemann, J. J. Testa, C. A. Emilio and M. I. Litter, *J. Photochem. Photobiol., A*, 2002, **148**, 223.
- J. Kim, J. Lee and W. Choi, *Chem. Commun.*, 2008, 756.
- C. Minero, G. Mariella, V. Maurino, D. Vione and E. Pelizzetti, *Langmuir*, 2000, **16**, 8964.
- H. Park and W. Choi, *J. Phys. Chem. B*, 2003, **107**, 3885.
- J. Theurich, M. Lindner and D. W. Bahnemann, *Langmuir*, 1996, **12**, 6368.
- M. I. Franch, J. Peral, X. Domenech and J. A. Ayllon, *Chem. Commun.*, 2005, 1851.
- S. Weon and W. Choi, *Environ. Sci. Technol.*, 2016, **50**, 2556.

